

New Adventures in Soft X-ray Scattering

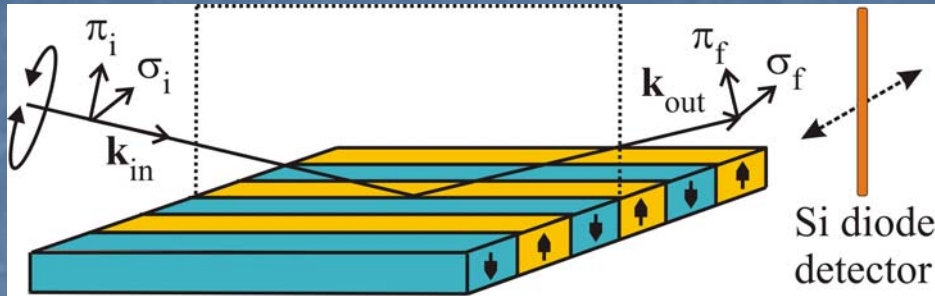
S.S. Dhesi

Diamond Light Source

Outline

- Soft X-ray Scattering from Stripe Domains
- Orbital ordering in $\text{La}_{0.5}\text{Sr}_{1.5}\text{MnO}_4$
- Future opportunities
- Summary

Soft X-ray Resonant Magnetic Scattering (SXRMS) from Stripe Domains



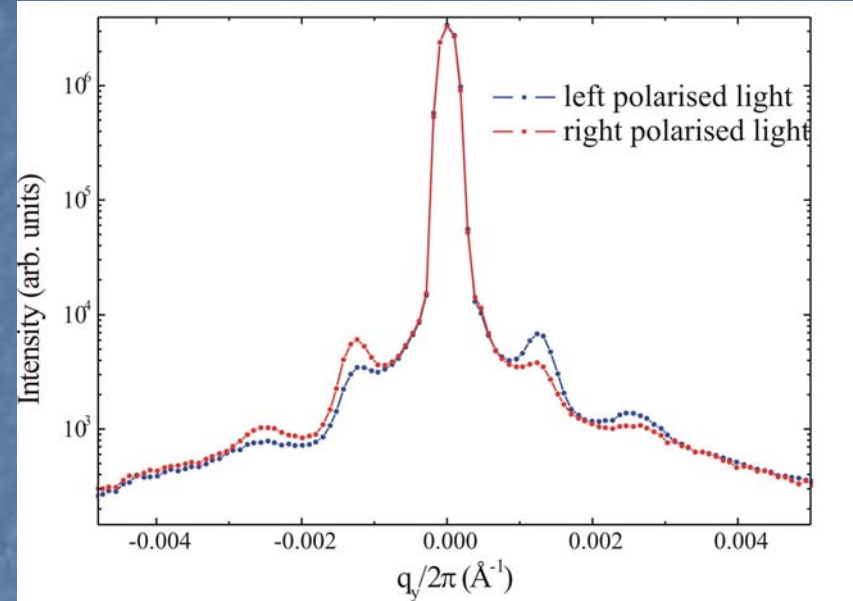
$$I \propto \left| \sum_n \exp(i\mathbf{q} \cdot \mathbf{r}_n) f_n \right|^2$$

$$f_n = \hat{\mathbf{e}}_f \cdot \hat{\mathbf{e}}_i F^0 - i(\hat{\mathbf{e}}_f \times \hat{\mathbf{e}}_i) \cdot \mathbf{M}_n F^1 + (\hat{\mathbf{e}}_f \cdot \mathbf{M}_n)(\hat{\mathbf{e}}_i \cdot \mathbf{M}_n) F^2$$

$\pi_f \rightarrow \sigma_i$ bulk domains

 $\sigma_i \rightarrow \pi_f$ bulk domains

$\pi_i \rightarrow \pi_f$ closure domains



SXRMS from stripe domains
in FePd films

SXRMS Scattering Amplitude

$$f_n = \hat{\mathbf{e}}_f \cdot \hat{\mathbf{e}}_i F^0 - i(\hat{\mathbf{e}}_f \times \hat{\mathbf{e}}_i) \cdot \mathbf{M}_n F^1 + (\hat{\mathbf{e}}_f \cdot \mathbf{M}_n)(\hat{\mathbf{e}}_i \cdot \mathbf{M}_n) F^2$$

Specular

1st order
SXRMS

2nd order
SXRMS

Linear in \mathbf{M}
XMCD

Quadratic in \mathbf{M}
XMLD

The $F^{1,2,3}$ terms can be decomposed into single particle operators just as in the case of the XMCD and XMLD sum rules. F^1 is then related to L and S whereas F^2 is related to the anisotropy of the spin-orbit interaction.

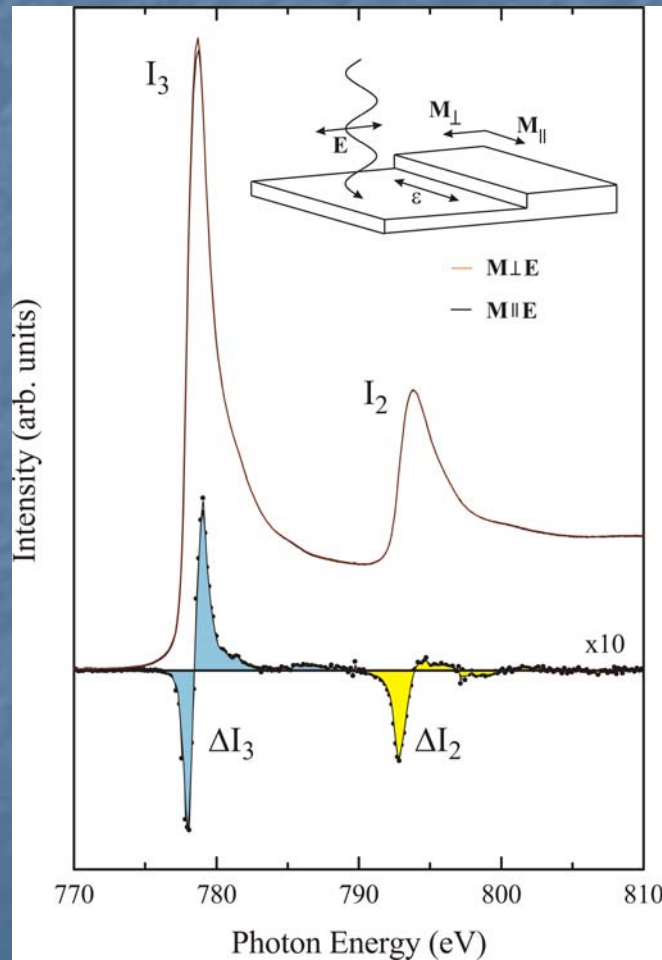
Hannon *et al.* Phys. Rev. Lett. 61, 1245 (1988).

Luo *et al.* Phys. Rev. Lett. 71, 287 (1993).

E. Dudzik *et al.* Phys. Rev. B 62, 5779 (2000).

X-ray Magnetic Linear Dichroism from stepped Co

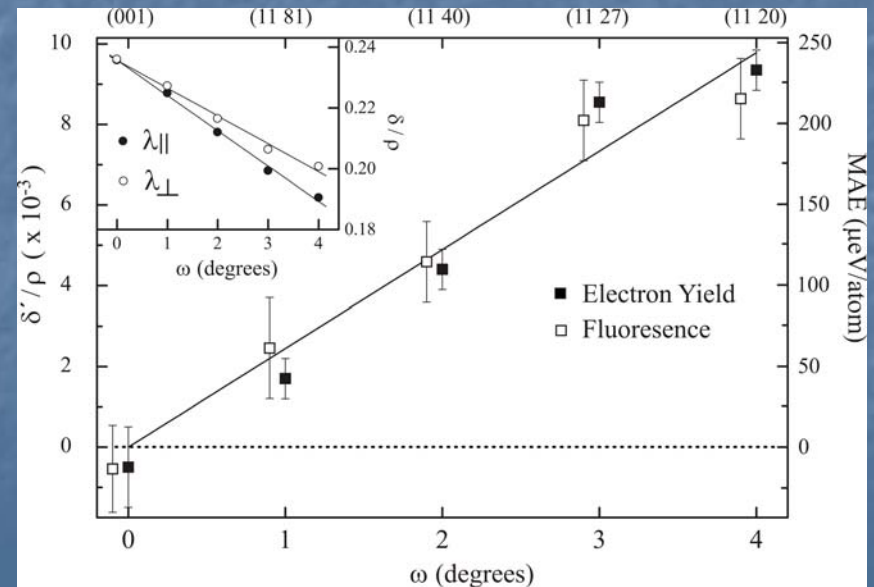
Vicinal Co MAE as a function of step density was determined using XMLD. The linear relationship between the step density and the MAE proves that XMLD is a measure of the MAE.



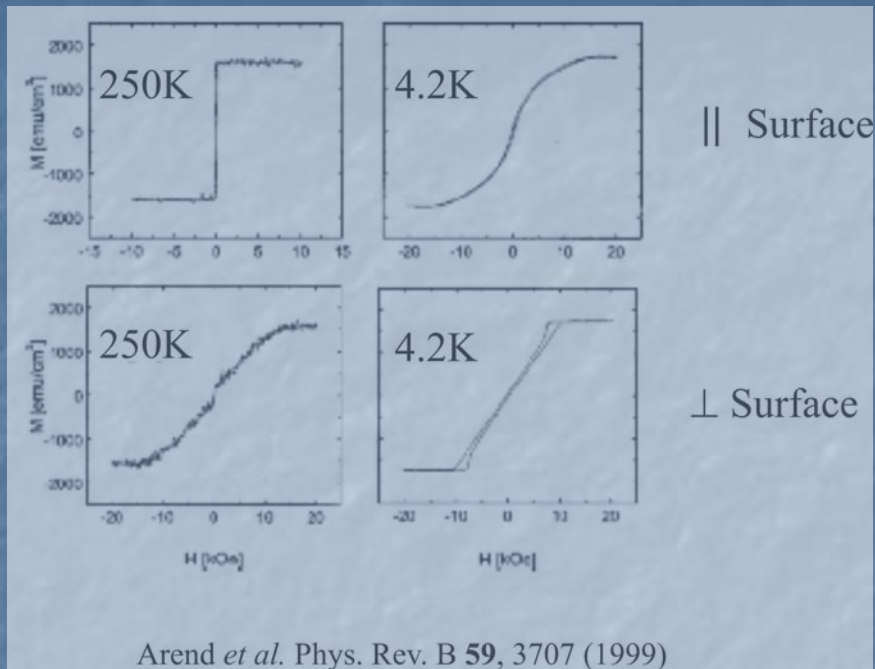
$$\delta' = \Delta I_3 - 2\Delta I_2 \quad \frac{\delta'}{\rho} = \frac{8\sqrt{3} \lambda_a}{5 n_h}$$

$$\rho = I_3 + I_2$$

$$\text{MAE} = \frac{1}{2}\zeta\langle\lambda_a\rangle$$



Magnetization curves of Fe/CeH₂ multilayers



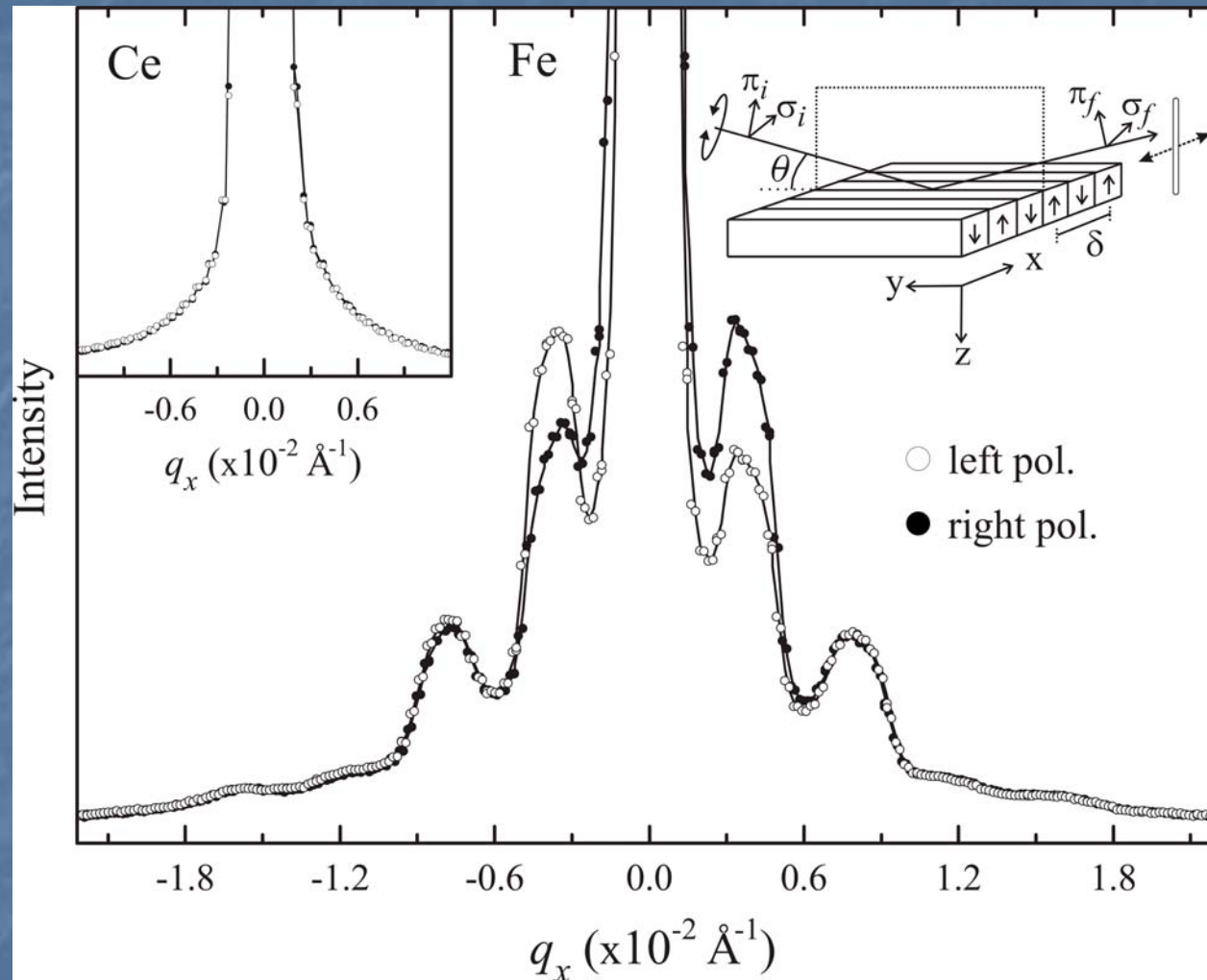
At 250K the easy-axis of magnetization is in-plane. At 4.2K the small remanent magnetization implies a multidomain configuration magnetized up and down along the surface normal. The MAE competes with the magnetostatic anisotropy arising from dipolar interactions to produce perpendicular domains, but where does the perpendicular MAE come from?

Single ion anisotropy:

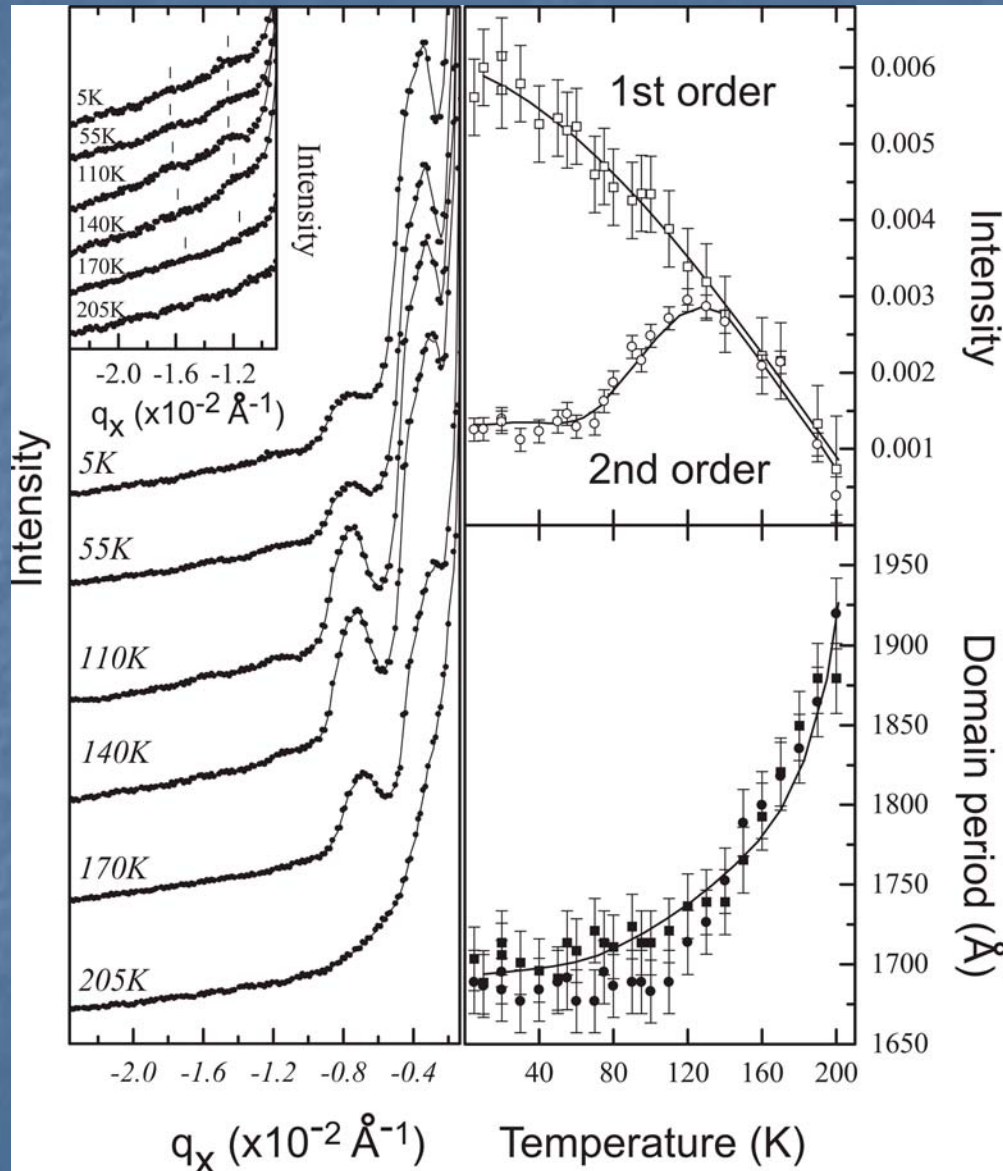
The Fe 3d spins moments polarize the Ce 5d states. This process leads to the magnetic polarization of the Ce 4f states.

However, the Fe 3d interface MAE could drive the spin reorientation without the single ion anisotropy

SXRMS from Fe/CeH₂ multilayers at 10K at the Fe L₃ edge



Temperature dependence of SXRMS at the Fe edge



Domain width

$$\delta = \frac{2C\sqrt{\gamma l}}{M_s}$$

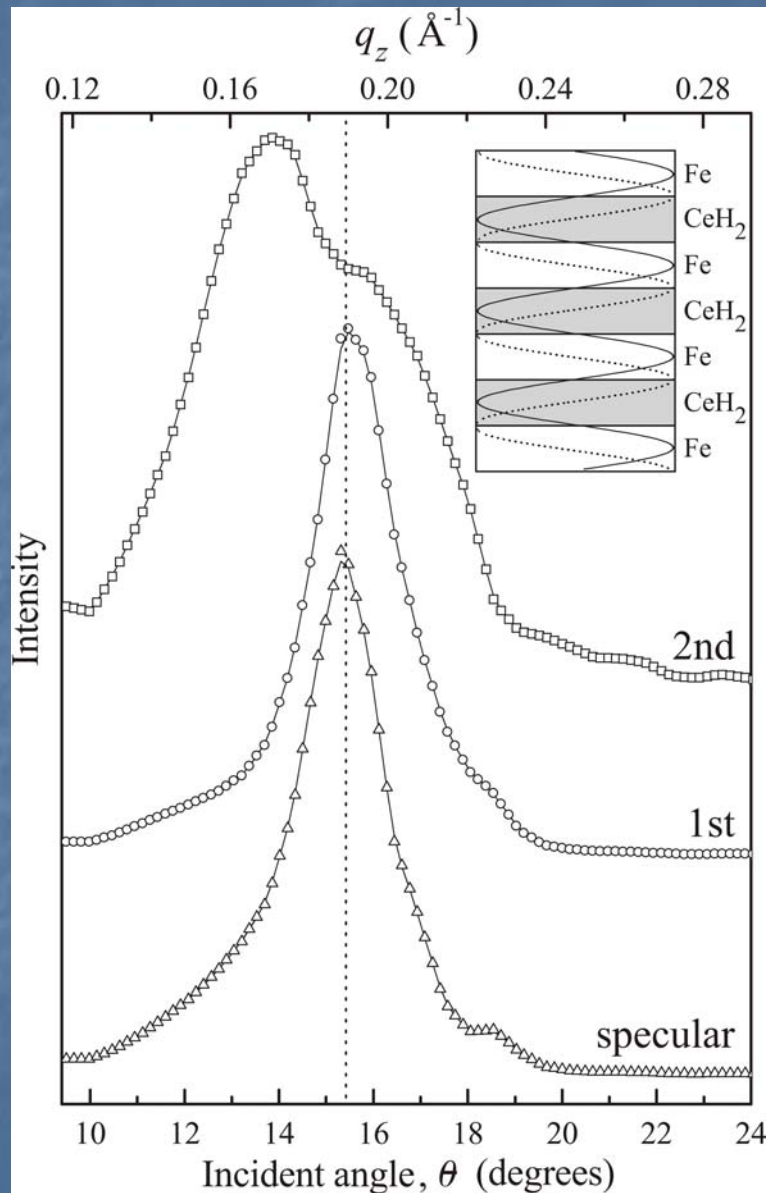
C = material constant
 l = multilayer thickness
 M_s = Sat. Magnetization
 γ = domain wall energy

$$\gamma = 4\sqrt{AK_u}$$

K_u = Uniaxial anisotropy
 (MAE)

A = Exchange stiffness

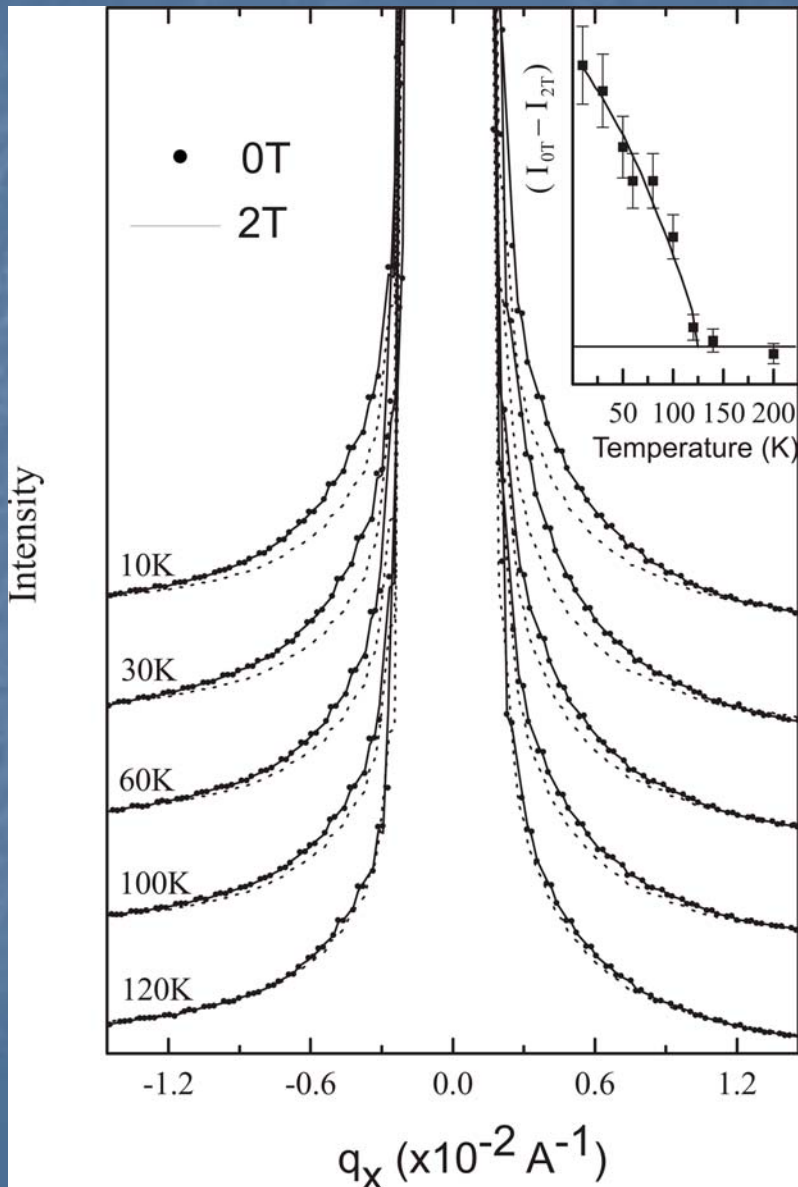
Intensity of the Bragg peak at the Fe edge



Intensity changes of the SXRMS features as the wavevector is scanned through the Bragg condition. The 2nd order feature clearly shows an angular shift. This shift arises from soft x-ray standing waves with their maxima at the interfaces.

The different angular dependence of the magnetic satellites demonstrates that the 1st and 2nd order contributions probe magnetic properties localized at the bulk Fe and interface Fe sites, respectively.

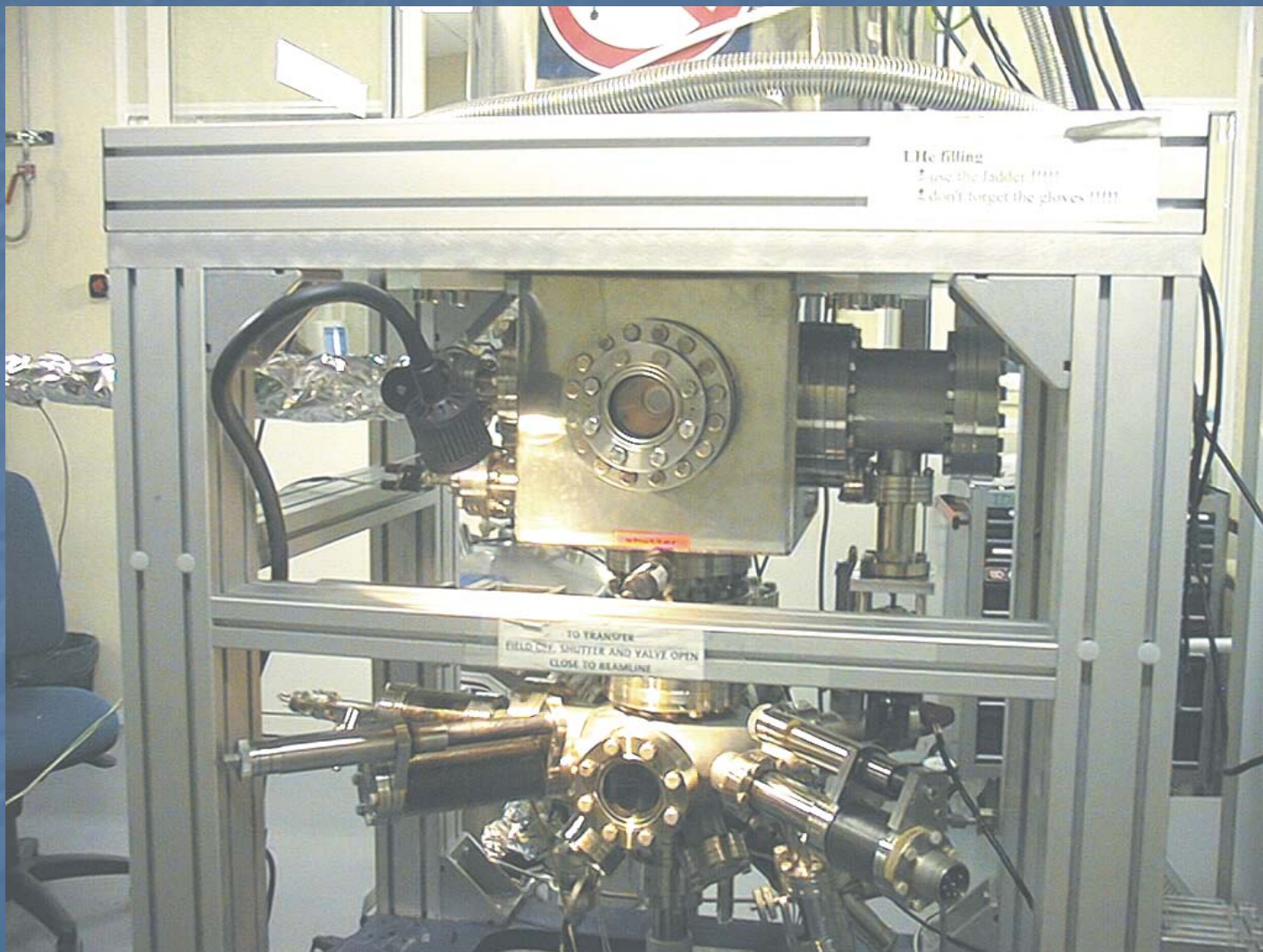
Temperature dependence of SXRMS at the Ce edge



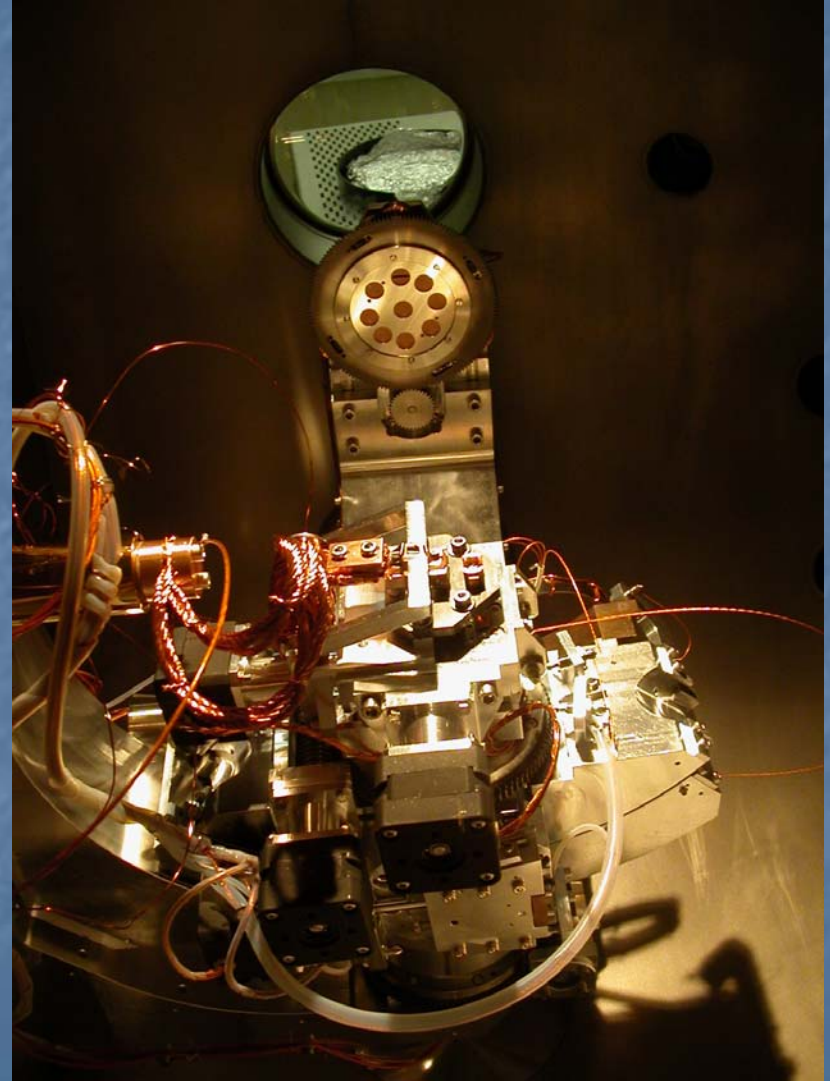
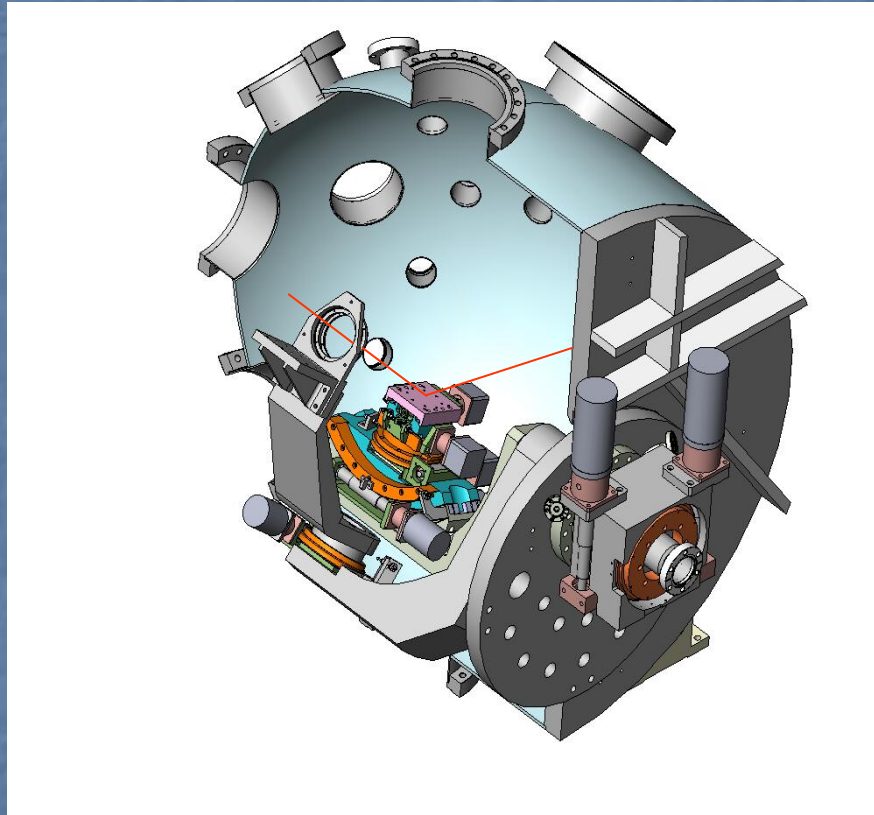
Temperature dependence of SXRMS features at the Ce M_5 edge.

The Ce SXRMS scattering features are absent until 120K indicating that the Fe $3d$ interface MAE controls the spin reorientation transition.

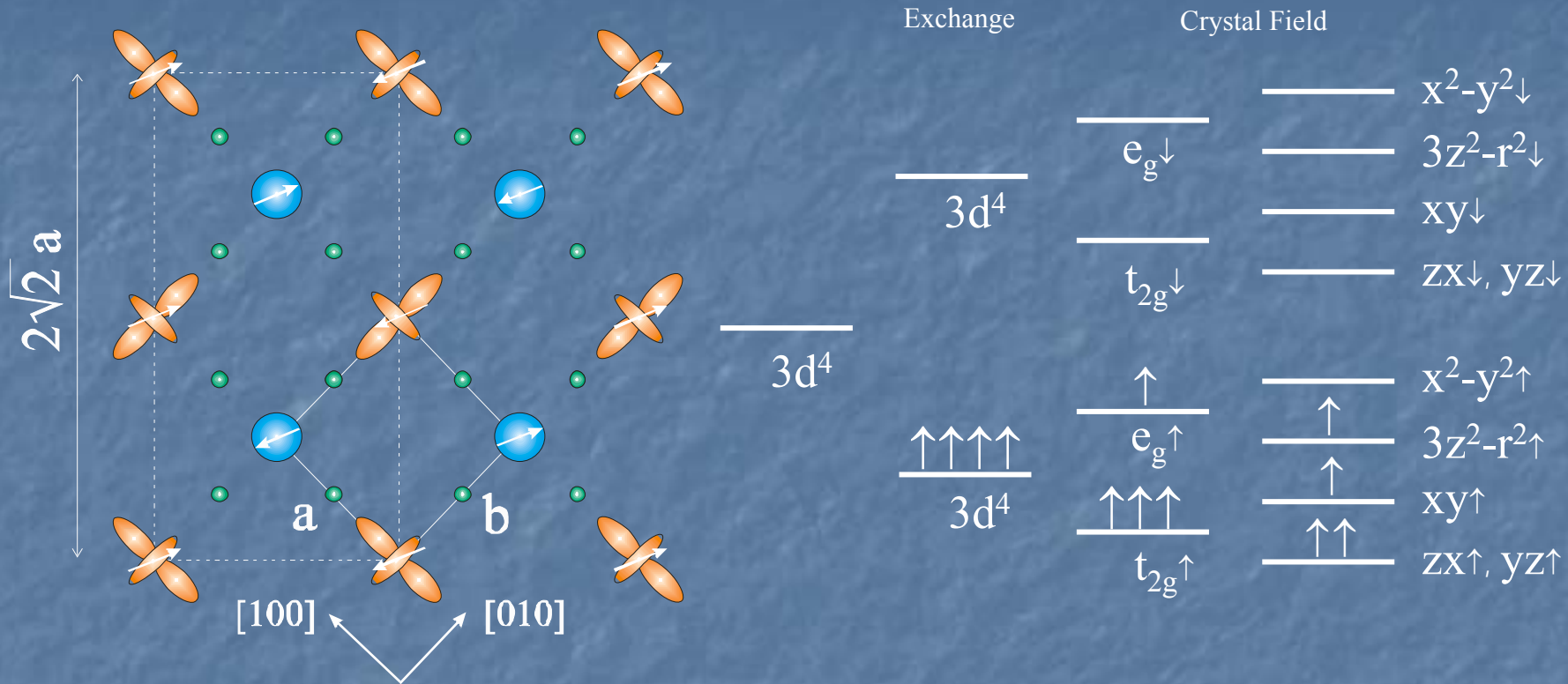
Soft X-ray Scattering experimental setup in the 7T magnet



ESRF ID8 Diffractometer



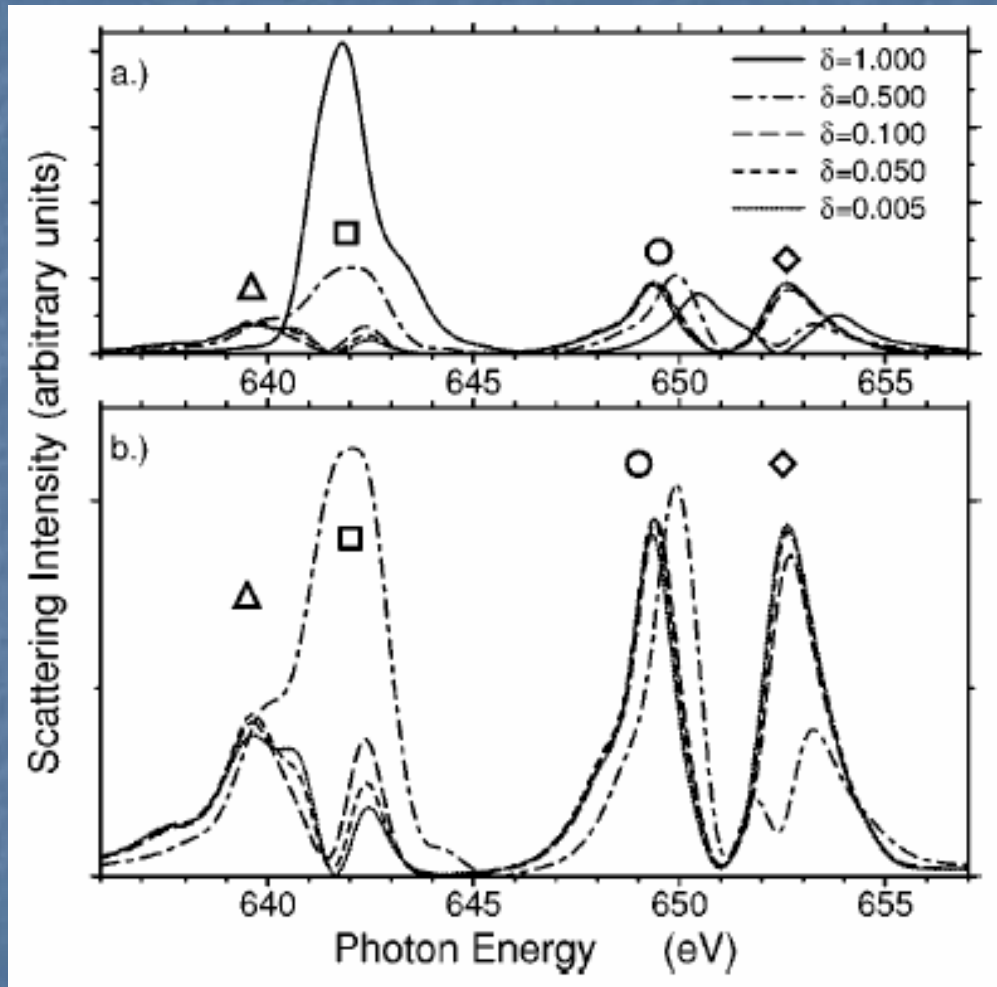
Orbital ordering in $\text{La}_{0.5}\text{Sr}_{1.5}\text{MnO}_4$



Hard x-ray resonant magnetic scattering has observed orbital ordering using $s \rightarrow p$ dipole transitions at the Mn K-edge. The sensitivity to the orbital ordering in the Mn $3d$ states was argued to be due to $4p-3d$ Coulomb interactions and Jahn-Teller distortions.

Y. Murakami *et al.* Phys. Rev. Lett. **80**, 1932 (1998).

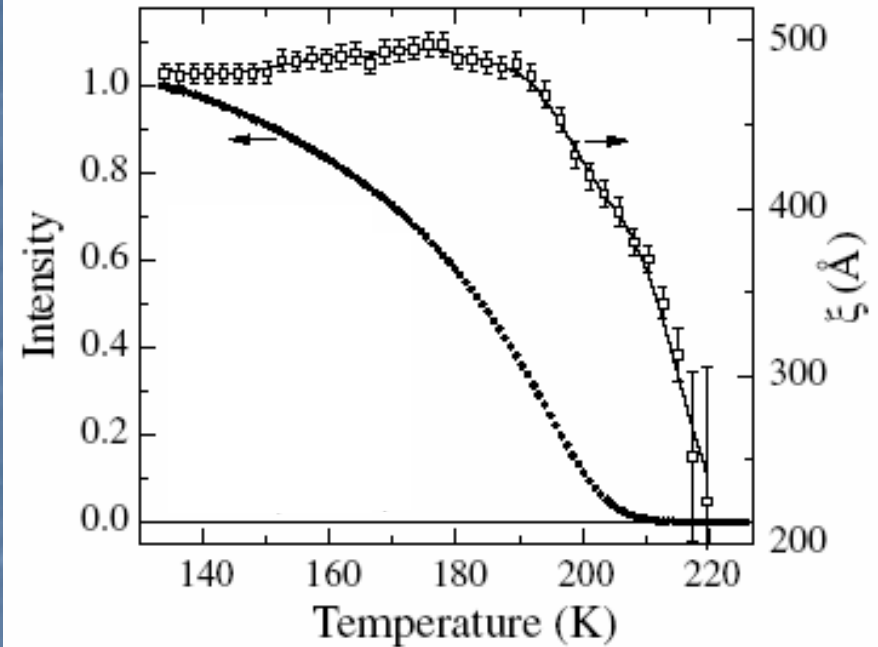
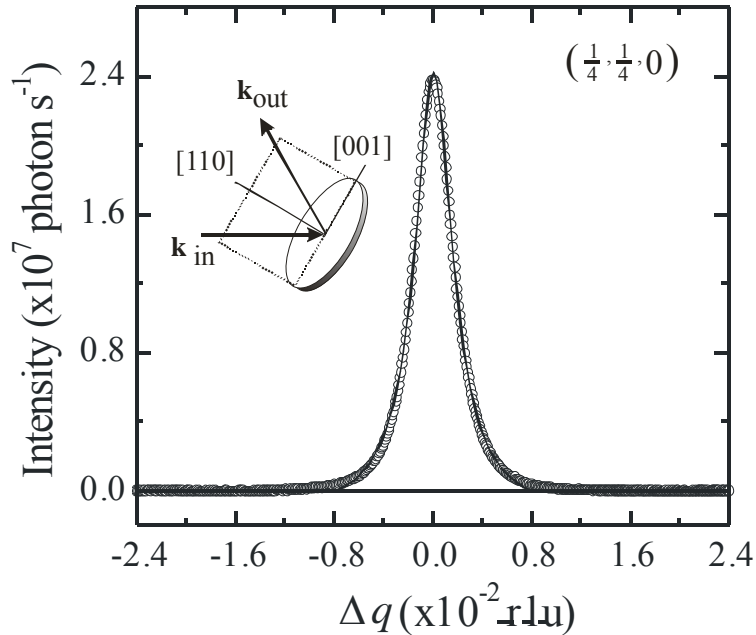
Orbital ordering in $\text{La}_{0.5}\text{Sr}_{1.5}\text{MnO}_4$



Castleton and Altarelli have proposed a method of separating orbital ordering from Jahn-Teller effects by measuring resonant scattering at the Mn $L_{2,3}$ edges. The energy dependence of the diffraction peak has a specific lineshape depending on the degree of Jahn-Teller distortions.

C. W. M. Castleton and
M. Altarelli
Phys. Rev. B 62, 1033 (2000)

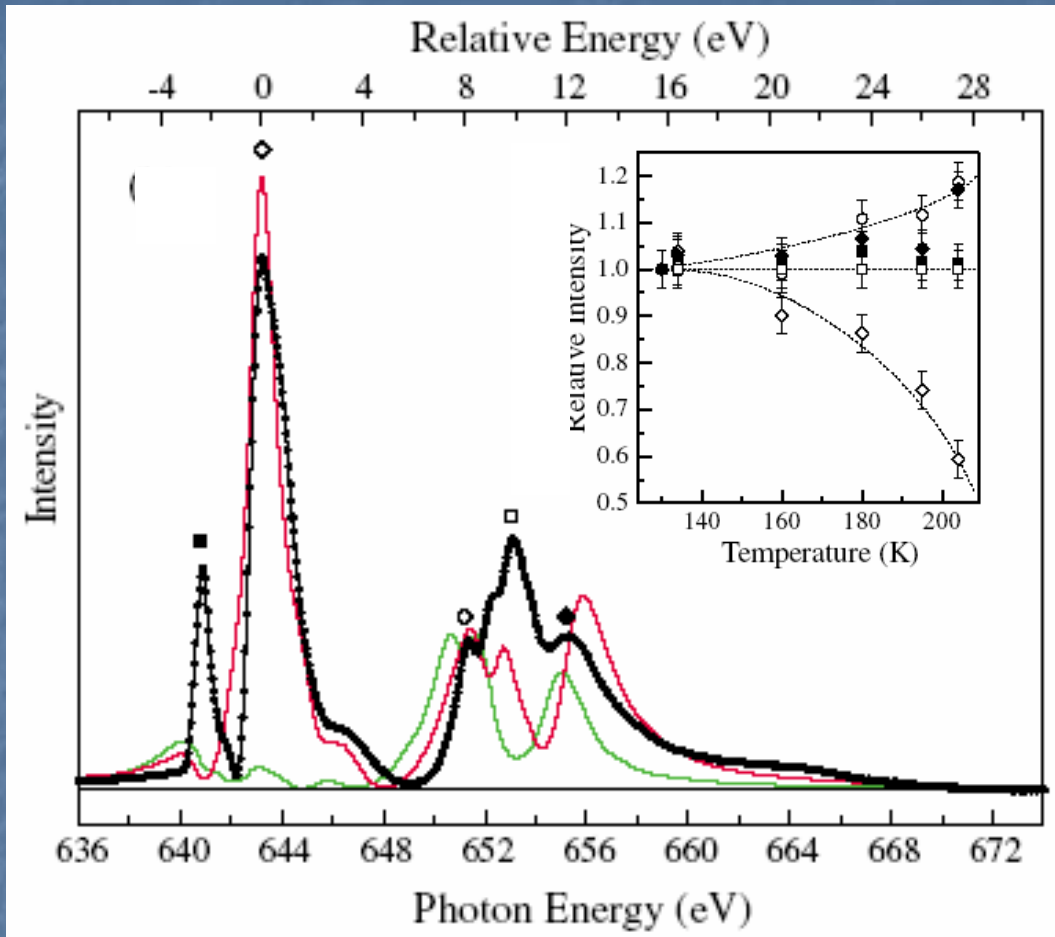
Orbital ordering in $\text{La}_{0.5}\text{Sr}_{1.5}\text{MnO}_4$



The forbidden reflection arising from orbital ordering recorded at the Mn L_3 edge.

The temperature dependence and correlation length, determined using the HWHM of the forbidden reflection.

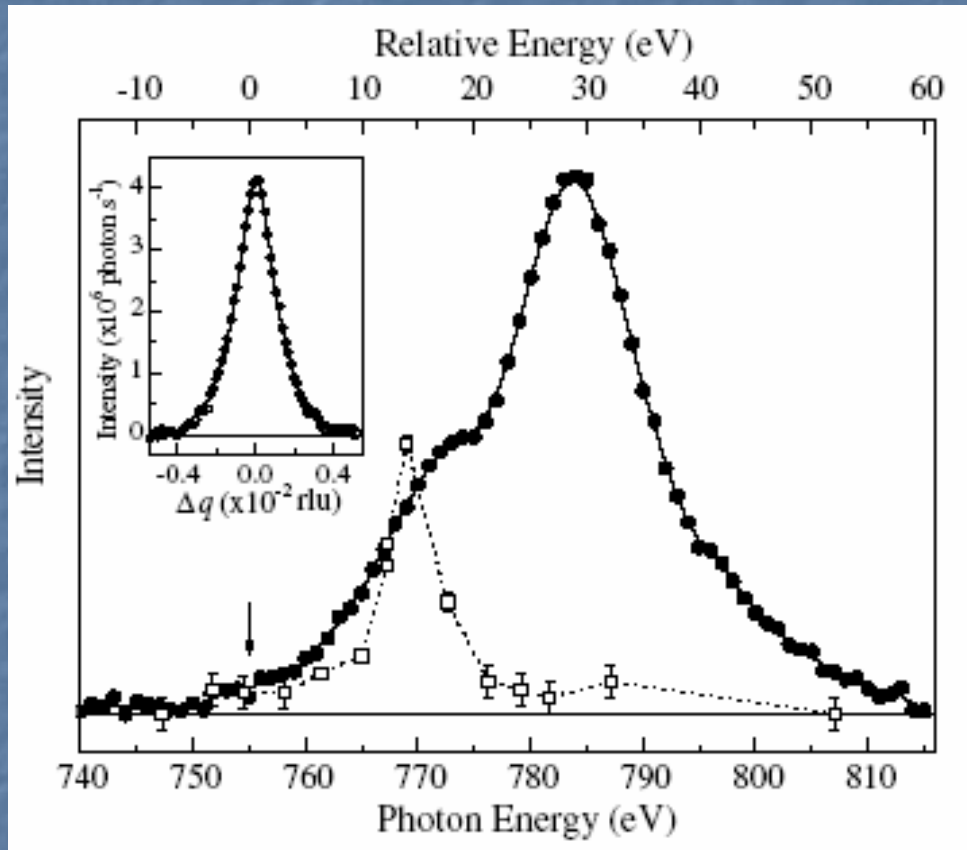
Orbital ordering in $\text{La}_{0.5}\text{Sr}_{1.5}\text{MnO}_4$



The black lines shows the experimental energy dependence of the forbidden reflection. The red line represents a ligand-field calculation for large Jahn-Teller distortions. The green line shows the same calculations for much smaller Jahn-Teller distortions.

The temperature dependence of the peaks is different implying that all the features in the energy dependence do not share a common origin.

Orbital ordering in $\text{La}_{0.5}\text{Sr}_{1.5}\text{MnO}_4$



The forbidden reflection arising from orbital ordering recorded at the Mn L_1 edge which involves $2s \rightarrow 4p$ transitions.

The energy dependence is distinctly different to that observed for the K-edge
Y. Murakami *et al.*

Phys. Rev. Lett. **80**, 1932 (1998)

Soft X-ray Scattering Facility

A multipurpose facility to study magnetic multilayers, manganites, superconductors, nanomagnetism and coherent diffraction.

Energy Range : 250 – 2000eV, optimised for 500-1000eV

Energy Resolution : ~5000

Spot Size : 50 μ m (H) x 50 μ m (V)

End station : uhv compatible 4 circle goniometer, SOC ~40 μ m

Modest angular resolution (0.0005 $^\circ$ for ϑ and 2ϑ)

Easy access to sample stage

Low temperatures (<20K)

Area detector, diode and sample drain current

Polarisation analysis, energy resolving

Pinhole for coherent diffraction, IFXS

Sample preparations chamber – cleaving, annealing

Alignment facilities (laser)

Aknowledgements

Beamline ID08, ESRF

N.B. Brookes

P. Bencok

C. DeNadai

F. Venturini

K. Larsson

G. van der Laan

A. Mirone

A. Tagliaferri

O. Toulemonde

E. Dudzik

H.A. Dürr

M. Münzenberg

W. Felsch

P. Ohresser

P. Reutler

A. Revcolevschi



Kenneth Larsson
1957 - 2004

Summary

Soft x-ray resonant magnetic scattering combined with soft x-ray standing waves is sensitive to the interface MAE and has been used to study the competing MAE contributions during a spin reorientation transition in Fe/CeH₂ multilayers

Orbital ordering in La_{0.5}Sr_{1.5}MnO₄ has been studied using soft x-ray diffraction at the Mn L_{2,3} edges. The results show that Jahn-Teller distortions are significant, but there is also evidence for orbital ordering distinct from the Jahn-Teller distortions.

Soft X-ray Resonant Magnetic Scattering and Soft X-Ray Resonant Diffraction will lead to new insights...and new problems.